Heavy ion escape from Martian wake enhanced by magnetic reconnection

Lei Wang
Institute of Geology and Geophysics, Chinese Academy of Sciences
Can Huang (huangcan@mail.iggcas.ac.cn)
Department of Geophysics and Planetary Science, University of Science and Technology of China
Yasong Ge
Institute of Geology and Geophysics, Chinese Academy of Sciences
A. M. Du
Rongsheng Wang
University of Science and Technology of China https://orcid.org/0000-0002-9511-7660
Tielong Zhang
Institute of Space Science and Applied Technology, Harbin Institute of Technology, Shenzhen
Jinqiao Fan
Institute of Geology and Geophysics, Chinese Academy of Sciences

Article

Keywords:

Posted Date: September 22nd, 2021

DOI: https://doi.org/10.21203/rs.3.rs-902571/v1

Abstract

How ion escape from the near-Mars space is one of the biggest puzzles for understanding the atmospheric evolution of Mars. Ions in the plasma wake region continuously escape from the unmagnetized planet. Although the average ion escape rate in the wake region is relatively low, observations also have revealed the presence of events that contribute bursty and enhanced ion escape fluxes. Boundary instabilities and magnetic reconnection are suggested to be the candidate mechanisms. However, there is a lack of evaluation of ion escape caused by reconnection and comparison of the two mechanisms under a similar plasma environment. Here, we show an exciting reconnection event in the Martian wake. Two types of flux ropes are observed during the event. One was generated by reconnection, while others were produced by dayside boundary instability and convected to tail. The escape rate of oxygen ions in the reconnection region was estimated to be about 53–72% of the total tailward escape. Furthermore, the escape flux in the flux rope produced by reconnection was over twice that caused by dayside instabilities.

Background

Mars has no global magnetic field[8]. As a consequence, the solar wind interacts directly with its upper atmosphere and ionosphere. The solar wind erosion of the Martian atmosphere may explain the dehydration of present-day Mars. Ion escape, in particular, through magnetotail or plasma wake, is a significant part of Martian atmospheric escape[9,10]. The main ion escape channels for Mars involve polar wind, boundary layer, ion pick-up, and plasma sheet[2,11]. Ion escape through the tail or wake region, however, should be inefficient because of Mars' obstruction. It has been reported that bursty and efficient ion escape processes exist in tail regions[4]. A similar process occurs in the Venusian tail[7], suggesting this process should be a common characteristic of unmagnetized planets.

Magnetic reconnection is a fundamental process that explosively dissipates magnetic energy[12] and depletes celestial bodies' charged particles, resulting in phenomena such as solar coronal mass ejection[13], disconnection of the comet tail[14], and atmospheric ion loss in planets[15]. Magnetic flux ropes often are identified in reconnection exhaust and diffusion region[16,17], with scales ranging from electron inertial length[18] to ion inertial length[19]. They wrap substantial plasma and cause large-scale ion escape during their release from the planetary tail[7]. Such flux rope structures can also form in the Martian dayside ionosphere from macroscopic instabilities because of the plasma flow shear and subsequently can be dragged into the tail[20,21]. Thus, to evaluate the role of magnetic reconnection for ion escape, it is necessary to assess the ion content within flux ropes of different origins. We first report the two types of flux ropes observed simultaneously during a single crossing of the Martian magnetotail current sheet (Fig. 1). The oxygen ion escape flux within the flux rope generated by the reconnection was more than twice that formed by boundary instabilities.

Results

One Martian current sheet crossing event. On 1 March 2021, the Mars Atmosphere and Volatile EvolutioN (MAVEN) orbiter[22] experienced a southward crossing of the tail current sheet. It successively grazed three flux ropes, as depicted in Fig. 1a. The spacecraft was located in the near-Mars tail at around [-1.2, 0.7, 0.4] R_M (radius of Mars, $1R_M$ = 3389.5 km) in the Mars-centered Solar Orbital (MSO) coordinates. The Magnetometer (MAG)[23] observed a reversal in the B_x component (Fig. 2b) and simultaneously a dip of $|B|$ (Fig. 2a) at 10:14:33 UT, indicating that MAVEN crossed the tail current sheet. The crustal magnetic field obtained from the spherical harmonic model[24] was vanishingly small throughout the interval (Fig. 2a). The energetic ion (up to a few hundreds of eV) population shown in Fig. 2e also implies that MAVEN crossed the current sheet[9,25]. Figure 2c shows that the current sheet was embedded in a relatively wide channel of plasma flow mainly in the anti-sunward direction. The Suprathermal and Thermal Ion Composition (STATIC)[26] instrument recorded multiple ion species, including , and across the current sheet (Fig. 2f). Heavy ions were more abundant than protons (Fig. 2d).

Referring to Fig. 2a, three evident local magnetic field enhancements were detected during the current sheet crossing. Meanwhile, distinct bipolar variations in the B_z component appeared around $|B|$ peaks (Fig. 2b), showing the characteristic features of flux ropes. For convenience, we name the three flux ropes FR1, FR2, and FR3. Note that the axial core field of FR1 and FR3 was mainly in the x-direction, while FR2 mainly aligned with the y-direction, implying that FR1 and FR3 may have different origins with FR2.

Magnetic reconnection and flux rope embedded in current sheet. As shown in Fig. 3, we investigate the MAVEN measurements within the overall current sheet (CS) coordinates. Figure 3a presents the magnetic field components ($\mathbf{B}_{CS}$) in the CS frame. Zooming in on the cross-tail component of the magnetic field (B_{MCS}), it is identified that asymmetric reversal signatures of B_{MCS} were prominent around the center plane of the tail current sheet. From 10:13:08 to 10:16:04 UT, we observed high-speed proton flow (V_L) up to 100 km/s (Fig. 3b). This speed was comparable to the Alfvén velocity in the adjacent lobe region (Fig. 3c), signaling that the proton flow was the outflow in the reconnection exhaust[27,28]. Such tailward proton flow and the negative B_{NCS} suggest that the reconnection site was on the sunward side of the MAVEN path (as indicated in Fig. 1b). In collisionless magnetic reconnection, Hall currents usually are directed toward the X-line along the magnetic field lines just inside the separatrices and away from the X-line along the separatrices[29,30]. Such a current system leads to a quadrupole Hall magnetic field. Theoretically, the Hall magnetic fields should show a bipolar variation from negative to positive if the spacecraft crossed the diffusion region along the $-\mathbf{N}_{CS}$ direction on the tailward side of the X-line. The observed B_{MCS} variations, as shown in Fig. 3a, are in good agreement with this theory. The Hall field was asymmetric because of the guide field along the $-\mathbf{M}_{CS}$ direction. The ambient reconnection field was about five times over the weak guide field after 10:17:00 UT. The asymmetric Hall magnetic field signature (B_{MCS}) combined with Alfvénic proton outflow are indicative of a component magnetic reconnection.

During 10:14:51–10:15:26 UT (shadowed region), FR2 traversed MAVEN quickly along the $-\mathbf{L}_{CS}$ and $-\mathbf{M}_{CS}$ directions. Meanwhile, a distinct polarity reversal was found in the $\mathbf{N}_{CS}$ direction, while a unimodal peak was found in the $\mathbf{M}_{CS}$ direction (Fig. 3e). According to our method of determining the axial direction of a flux rope, the $\mathbf{M}_{FR2}$ axis is adopted as the FR2 axial direction. The angle between $\mathbf{M}_{FR2}$ and $\mathbf{M}_{CS}$ axis was about 162°, that is, the axial core field of FR2 was approximately antiparallel to the $\mathbf{M}_{CS}$ direction or was along the reconnection guide field. These observations are consistent with a flux rope formed by magnetotail reconnection[31,32]. Figure 3f exhibits the electron differential energy flux from the Solar Wind Electron Analyzer (SWEA)[33]. Enhancements of energetic electron flux above 500 eV can be seen during the crossing of the current sheet. Time slices of the electron energy spectrum near core regions of three flux ropes are provided in Fig. 3g–i. The spectrum shapes in these regions are different. Electron spectra within FR1 and FR3 displayed approximate Maxwellian distributions. For FR2, however, there was a flat-top population between 150 eV and 320 eV superimposed on a Maxwellian distribution, which is a typical feature of magnetic reconnection exhaust[34,35]. Moreover, suprathermal (300–800 eV) electrons substantially increased within FR2. This combined evidence indicates that FR2 was generated by reconnection and expelled quickly from the X-line in the exhaust.

Flux ropes on the edge of current sheet. We also perform an MVA analysis on the magnetic field measurements of FR1 and FR3 (Fig. 4). The axes of FR1 and FR2 were $\mathbf{L}_{FR1}$ = [0.68, -0.43, -0.59] and $\mathbf{M}_{FR3}$ = [-0.89, -0.24, -0.39], respectively (Fig. 4a, c). Both axes were quasi-perpendicular (128° and 119°) to the cross-tail direction of the current sheet. Hodograms on the L_{FR}-M_{FR} plane show that the magnetic field variations of FR1 occured mainly in quadrants 1 and 4 and rotated clockwise (Fig. 4b), whereas that of FR3 occured mainly in quadrants 1 and 2 and rotated counterclockwise (Fig. 4d). Because the signs of are positive for both of them, the helicity of FR1 and FR3 are left-handed and right-handed, respectively. The quasi-perpendicularity between the axis and $\mathbf{M}_{CS}$, as well as the opposite helicities of the flux ropes on either side of the current sheet, suggesting that they may be generated by dayside ionospheric instabilities and dragged into the tail by the solar wind[36,37].

To compare the MAVEN observations with the theoretical prediction, we study the configuration of magnetic field lines hanging on the dayside ionosphere. In this event, MAVEN traveled from the nominal bow shock and magnetic pile-up boundary to the site adjacent to the current sheet during 09:05:00–10:10:00 UT (see Supplementary Fig. 1). Four snapshots of the magnetic field clock angle in the M_{CS}-N_{CS} plane are shown along the orbit. During this time, the clock angle changed less than ±15° from the Martian magnetosheath to the tail current sheet, suggesting that the orientation of the incoming and hanging interplanetary magnetic field (IMF) barely changed in the M_{CS}-N_{CS} plane. The magnetic field vector on the M_{CS}-N_{CS} plane was approximately along the $-\mathbf{N}_{CS}$ direction after MAVEN was deep into the near-Mars induced magnetosphere. The FR1 event was observed by the spacecraft in the $+\mathbf{M}_{CS}$ hemisphere. As shown in the schematic (Fig. 1c), the velocity shear between the magnetosheath and the ionosphere could lead to field line twisting and rolling up to form a flux rope. In this scenario, the twisted field lines on the two sides of the current sheet rotate in opposite directions. The observed opposite

helicities of FR1 and FR3 are in good agreement with this theoretical prediction, given that FR1 and FR3 were observed on both sides of the current sheet.

Discussion

The mean tailward ion fluxes in the reconnection exhaust region were about 2.7×10^6 $cm^{-2}s^{-1}$ and 3.7×10^6 $cm^{-2}s^{-1}$ for and , respectively (Fig. 3d). The fluxes are clearly enhanced compared to the mean tailward flux[38]. We estimate the escape rate during this reconnection (3.9×10^{23} s^{-1}) to be about 22–30% of the average tailward ion escape rate ($1.3–1.8\times10^{24}$ s^{-1})[38], while (5.5×10^{23} s^{-1}) was about 31–42%. Thus, the heavy-ion escape through the reconnection outflow region is significant for Martian ion escape. Note that the observed densities (about 0.7 cm^{-3} for and 1.2 cm^{-3} for) of oxygen ions in this event are lower than that in the typical plasma sheet[39]. The oxygen ion escape caused by the reconnection in this study may even have been underestimated. The mean oxygen ion flux within FR1, FR2, and FR3 were 4.8×10^6 $cm^{-2}s^{-1}$, 1.1×10^7 $cm^{-2}s^{-1}$, and 4.0×10^6 $cm^{-2}s^{-1}$, respectively. The heavy ion escape rate in the flux rope generated by reconnection was also greater than that generated by boundary instabilities. In the current sheet normal direction, the spacecraft velocity was about -2.9 km/s, and the average proton velocity was about 3.6 km/s, so the half-width of the current sheet was about 720 km, given the crossing time was about 220 s. We also derive ion inertial lengths of ~620 km for (d_H), ~1180 km for and ~1250 km for from the average ion densities during the crossing of the current sheet (see Fig. 2d). Thus, this current sheet was as thin as the characteristic proton length that recently has been detected frequently[40-42]. Theoretically, magnetic reconnection can be triggered only after a current sheet becomes thinner than d_H[43], implying that magnetic reconnection in the Martian tail may occur more frequently and thus be critical to the Martian ion escape process. This enhancement of ion escape due to reconnection should also occur on other non-magnetized planets like Venus.

Methods

Local coordinate system for the current sheet and flux ropes. We obtain the local (LMN) coordinate system from the minimum variance analysis[44]. To obtain the overall current sheet coordinate system, we apply MVA on $\mathbf{B}_{CS}$ observed between 10:13:00 and 10:16:40, after removing the signals of the flux ropes from original data (where $\mathbf{B}_{CS} = \mathbf{B}\text{-}\mathbf{B}_{FR}$). This yields $\mathbf{L}_{CS}$ = [0.99, -0.12, 0.03], $\mathbf{M}_{CS}$ = [0.09, 0.85, 0.53], $\mathbf{N}_{CS}$ = [-0.08, -0.52, 0.85] relative to the MSO coordinates. During this event, the ion flow speed was much higher than the spacecraft on-orbit speed, corresponding to a crossing with the current sheet overtaking the spacecraft[45]. We determine the LMN coordinate by ensuring positive dot products between the $\mathbf{L}_{CS}$ direction and the sun direction, and negative dot products between the $\mathbf{N}_{CS}$ direction and the spacecraft velocity direction. The magnetic field of flux ropes were also transformed into respective local coordinate with $\mathbf{L} = [0.68, -0.43, -0.59]_{MSO}$, $\mathbf{M} = [0.39, -0.47, 0.79]_{MSO}$, and $\mathbf{N} = [-0.62, -0.77, -0.16]_{MSO}$ for FR1; $\mathbf{L} = [0.38, -0.47, 0.80]_{MSO}$, $\mathbf{M} = [-0.35, -0.87, -0.35]_{MSO}$, and $\mathbf{N} = [0.86, -0.15, -0.49]_{MSO}$ for FR2; and $\mathbf{L} = [-0.23, -0.50, 0.84]_{MSO}$, $\mathbf{M} = [-0.89, -0.24, -0.39]_{MSO}$, and $\mathbf{N} = [0.40, -0.83, -0.39]_{MSO}$ for FR3.

Calculation of axial orientation and handedness of a flux rope. This method is valid regardless of whether or not the flux rope is force-free and is based only on single-spacecraft measurements. According to characteristics of azimuthal and axial fields (bipolar for the azimuthal and unipolar for the axial) of flux ropes, we calculate in the flux rope LMN coordinate system, where ξ represents $\mathbf{L}_{FR}$ or $\mathbf{M}_{FR,}$ and j is the temporal index. The larger (smaller) one corresponds to the axial component (azimuthal component). We define the sign of the helicity as . The positive (negative) helicity means that the handedness of a flux rope was right-handed (left-handed). The term is the directional area on the B_L-B_M plane. Its magnitude denotes the integral area, and the positive (negative) sign denotes the $+\mathbf{N}_{FR}$ ($-\mathbf{N}_{FR}$) direction. The term means the sign of observed helicity is also associated with the relative trajectory of crossing. $\mathbf{V}_p$ and $\mathbf{V}_S$ are the velocities of the protons and the satellite, respectively.

Estimation of oxygen ions' escape rate. In the overall exhaust, oxygen ions mainly moved along the -**L** direction of the current sheet. Thus, we obtain fluxes of oxygen ions in the exhaust and diffusion regions by integrating the product of densities and V_L. To compare the flux of oxygen ions within the three flux ropes, it is reasonable to take the mean value of the product as an indicator. Estimating the cross-section of the exhaust is critical for calculating the ion escape rate. Observations have found that the length of the cross-tail current of Mars is even larger than the diameter of the planet[46]. We assume that the exhaust region extended to the length of the diameter of Mars. In the current sheet normal direction, we obtain the width of the exhaust by the time integration of the relative speed of the satellite and the current sheet. Because protons are more difficult to decouple from the magnetic field than oxygen ions, the velocity of protons could be used as a probe of the velocity of the current sheet.

Declarations

Data availability. The data analyzed in this study are available in NASA's Planetary Data System (https://pds-ppi.igpp.ucla.edu). The corresponding authors can also provide data supporting the plots within this paper and other finding of this research upon reasonable request.

Acknowledgments

We would like to acknowledge data supports from the MAVEN project team. This work is supported by the National Natural Science Foundation of China (41974173, 41674168, 41774176 and 41874080), Beijing Municipal Science and Technology Commission (Grant No. Z191100004319001), the pre-research Project on Civil Aerospace Technologies No. D020103 funded by CNSA, the Strategic Priority Research Program of Chinese Academy of Sciences (Grant No. XDA14040403, XDA14040404) and the Youth Innovation Promotion Association, Chinese Academy of Sciences.

Author contributions

L.W. and C.H. led the research and carried out the analysis of all of the observations. Y.S.G. contributed to scientific interpretation of the results and drafting of the manuscript. A.M.D. provided expertise on

magnetic field and current environments of Martian magnetotail. R.S.W. provided knowledge of magnetic reconnection. T.L.Z. participated in the analysis of the results. J.Q.F. participated in the development of the method of determining the sign of the helicity of a flux rope. All authors contributed to the presentation of the manuscript.

References

1. Barabash, S. *et al.* The loss of ions from Venus through the plasma wake. *Nature* 450, 650-653, (2007).

2. Dubinin, E. *et al.* Ion Energization and Escape on Mars and Venus. *Space Science Reviews* 162, 173-211, (2011).

3. Lundin, R. Ion Acceleration and Outflow from Mars and Venus: An Overview. *Space Science Reviews* 162, 309-334, (2011).

4. Dubinin, E. *et al.* Bursty escape fluxes in plasma sheets of Mars and Venus. *Geophysical Research Letters* 39, L01104, (2012).

5. Dubinin, E. et al. Bursty Ion Escape Fluxes at Mars. *Journal of Geophysical Research: Space Physics* 126, (2021).

6. Halekas, J. S. *et al.* Plasma clouds and snowplows: Bulk plasma escape from Mars observed by MAVEN. *Geophysical Research Letters* 43, 1426-1434, (2016).

7. Zhang, T. L. *et al.* Magnetic reconnection in the near Venusian magnetotail. *Science* 336, 567-570, (2012).

8. Acuna, M. H. *et al.* Magnetic Field and Plasma Observations at Mars: Initial Results of the Mars Global Surveyor Mission. *Science* 279, 1676-1680, (1998).

9. Dubinin, E., Lundin, R., Norberg, O. & Pissarenko, N. Ion acceleration in the Martian tail: Phobos observations. *Journal of Geophysical Research: Space Physics* 98, 3991-3997, (1993).

10. Barabash, S., Fedorov, A., Lundin, R. & Sauvaud, J. A. Martian atmospheric erosion rates. *Science* 315, 501-503, (2007).

11. Lillis, R. J. *et al.* Characterizing Atmospheric Escape from Mars Today and Through Time, with MAVEN. *Space Science Reviews* 195, 357-422, (2015).

12. Giovanelli, R. G. A Theory of Chromospheric Flares. *Nature* 158, 81-82, (1946).

13. Chen, P. F. Coronal Mass Ejections: Models and Their Observational Basis. *Living Reviews in Solar Physics* 8, (2011).

14. Russell, C. T., Saunders, M. A., Phillips, J. L. & Fedder, J. A. Near-tail reconnection as the cause of cometary tail disconnections. *Journal of Geophysical Research* 91, 1417, (1986).

15. Russell, C. T., Khurana, K. K., Huddleston, D. E. & Kivelson, M. G. Localized reconnection in the near jovian magnetotail. *Science* 280, 1061-1064, (1998).

16. Drake, J. F., Swisdak, M., Che, H. & Shay, M. A. Electron acceleration from contracting magnetic islands during reconnection. *Nature* 443, 553-556, (2006).

17. Chen, L. J. *et al.* Observation of energetic electrons within magnetic islands. *Nature Physics* 4, 19-23, (2007).

18. Wang, R. *et al.* Coalescence of magnetic flux ropes in the ion diffusion region of magnetic reconnection. *Nature Physics* 12, 263-267, (2015).

19. Eastwood, J. P. Observations of multiple X-line structure in the Earth's magnetotail current sheet: A Cluster case study. *Geophysical Research Letters* 32, (2005).

20. Wolff, R. S., Goldstein, B. E. & Yeates, C. M. The onset and development of Kelvin-Helmholtz instability at the Venus ionopause. *Journal of Geophysical Research* 85, 7697, (1980).

21. Elphic, R. C. & Russell, C. T. Evidence for helical kink instability in the Venus magnetic flux ropes. *Geophysical Research Letters* 10, 459-462, (1983).

22. Jakosky, B. M. et al. The mars atmosphere and volatile evolution (MAVEN) mission. Space Sci. Rev. 195, 3–48 (2015).

23. Connerney, J. E. P. *et al.* The MAVEN Magnetic Field Investigation. *Space Science Reviews* 195, 257-291, (2015).

24. Morschhauser, A., Lesur, V. & Grott, M. A spherical harmonic model of the lithospheric magnetic field of Mars. *Journal of Geophysical Research: Planets* 119, 1162-1188, (2014).

25. Dubinin, E. & Fraenz, M. Magnetotails of Mars and Venus. *Geophys. Monogr. Ser.* 207, 43-59, (2015).

26. McFadden, J. P. *et al.* MAVEN SupraThermal and Thermal Ion Compostion (STATIC) Instrument. *Space Science Reviews* 195, 199-256, (2015).

27. Wu, P. & Shay, M. A. Magnetotail dipolarization front and associated ion reflection: Particle-in-cell simulations. *Geophysical Research Letters* 39, L08107, (2012).

28. Huang, C., Lu, Q., Lu, S., Wang, P. & Wang, S. The effect of a guide field on the structures of magnetic islands formed during multiple X line reconnections: Two-dimensional particle-in-cell simulations. *Journal of Geophysical Research: Space Physics* 119, 798-807, (2014).

29. Oieroset, M., Phan, T. D., Fujimoto, M., Lin, R. P. & Lepping, R. P. In situ detection of collisionless reconnection in the Earth's magnetotail. *Nature* 412, 414-417, (2001).

30. Lu, Q. *et al.* Features of separatrix regions in magnetic reconnection: Comparison of 2-D particle-in-cell simulations and Cluster observations. *Journal of Geophysical Research: Space Physics* 115, A11208, (2010).

31. Eastwood, J. P., Videira, J. J. H., Brain, D. A. & Halekas, J. S. A chain of magnetic flux ropes in the magnetotail of Mars. *Geophysical Research Letters* 39, L03104, (2012).

32. Hara, T. *et al.* On the origins of magnetic flux ropes in near-Mars magnetotail current sheets. *Geophysical Research Letters* 44, 7653-7662, (2017).

33. Mitchell, D. L. *et al.* The MAVEN Solar Wind Electron Analyzer. *Space Science Reviews* 200, 495-528, (2016).

34. Asano, Y. *et al.* Electron flat-top distributions around the magnetic reconnection region. *Journal of Geophysical Research: Space Physics* 113, A01207, (2008).

35. Wang, R., Lu, Q., Li, X., Huang, C. & Wang, S. Observations of energetic electrons up to 200 keV associated with a secondary island near the center of an ion diffusion region: A Cluster case study. *Journal of Geophysical Research: Space Physics* 115, A11201, (2010).

36. Luhmann, J. G. & Cravens, T. E. Magnetic fields in the ionosphere of Venus. *Space Science Reviews* 55, (1991).

37. Wei, H. Y., Russell, C. T., Zhang, T. L. & Dougherty, M. K. Comparison study of magnetic flux ropes in the ionospheres of Venus, Mars and Titan. *Icarus* 206, 174-181, (2010).

38. Dong, Y. *et al.* Strong plume fluxes at Mars observed by MAVEN: An important planetary ion escape channel. *Geophysical Research Letters* 42, 8942-8950, (2015).

39. Inui, S. *et al.* Statistical Study of Heavy Ion Outflows From Mars Observed in the Martian-Induced Magnetotail by MAVEN. *Journal of Geophysical Research: Space Physics* 124, 5482-5497, (2019).

40. Harada, Y. *et al.* Magnetic reconnection in the near-Mars magnetotail: MAVEN observations. *Geophysical Research Letters* 42, 8838-8845, (2015).

41. Grigorenko, E. E. *et al.* Imprints of Quasi-Adiabatic Ion Dynamics on the Current Sheet Structures Observed in the Martian Magnetotail by MAVEN. *J Geophys Res-Space* 122, 10176-10193, (2017).

42. Grigorenko, E. E. *et al.* Thin Current Sheets of Sub-ion Scales observed by MAVEN in the Martian Magnetotail. *Geophysical Research Letters* 46, 6214-6222, (2019).

43. Fujimoto, K. Time evolution of the electron diffusion region and the reconnection rate in fully kinetic and large system. *Physics of Plasmas* 13, 072904, (2006).

44. Sonnerup, B. U. & Scheible, M. Minimum and Maximum Variance Analysis. *in Analysis Methods for Multi-spacecraft Data, edited by G. Paschmann and P. W. Dayly, pp. 185-220, ISSI SR-001, ESA Publ. Div., Noordwijk, Netherlands.*, (1998).

45. Harada, Y. et al. Survey of magnetic reconnection signatures in the Martian magnetotail with MAVEN. *Journal of Geophysical Research: Space Physics* 122, 5114-5131, (2017).

46. Ramstad, R. et al. The global current systems of the Martian induced magnetosphere. *Nature Astronomy* 4, 979-985, (2020).

Figures

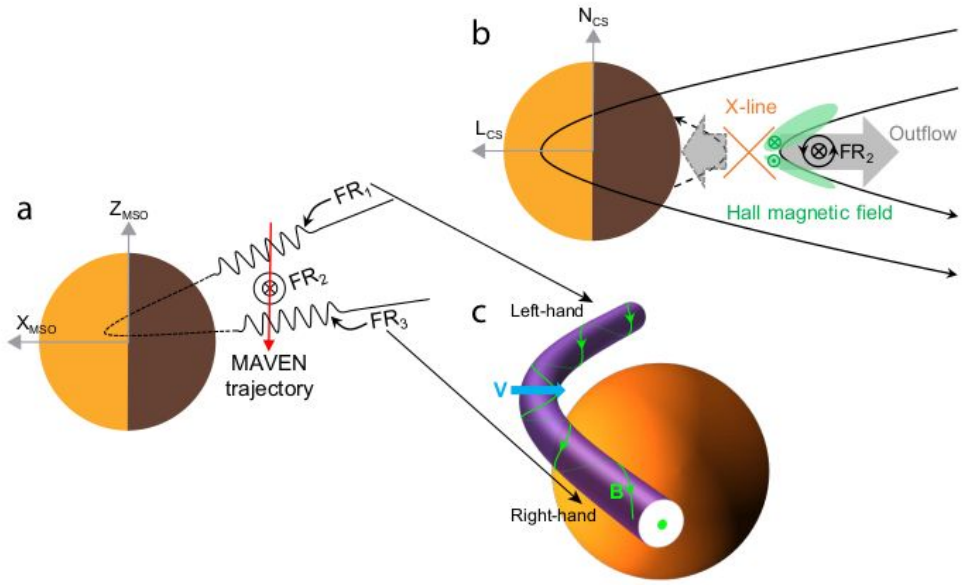

Figure 1

Schematic diagrams of flux ropes in the wake region oringined from magnetic reconnection and dayside boundary instability. (a) Sketch of MAVEN crossing of the current sheet and three flux ropes (abbreviated as FR1, FR2 and FR3, respectively). The red arrow denotes MAVEN trajectory. (b) Schematic of the reconnection occuring in the Martian tail current sheet. During the crossing, we observed Alfvénic tailward flow and asymetric Hall fields (green regions). The dashed line and dashed arrow represent the assumed

reconnected field line and outflow in the Marsward side of reconnection site in theory. Within the current sheet, reconnection produces the flux rope FR2. (c) FRs produced by boundary instability in the Martian dayside. The purple tube represents a magnetic flux tube, and the green line means the magnetic field line rolled up by the shear flow (the blue arrow). As a result, the handedness of the two sides of the twisted flux tube is opposite. The flux rope is dragged by the solar wind to the magnetotail, which corresponds to FR1 and FR3 on both sides of the current sheet. Note that we cannot tell if FR1 and FR3 were connected to a same magnetic field line or combined in a same flux tube, as shown in Fig. 1a with the dashed segment.

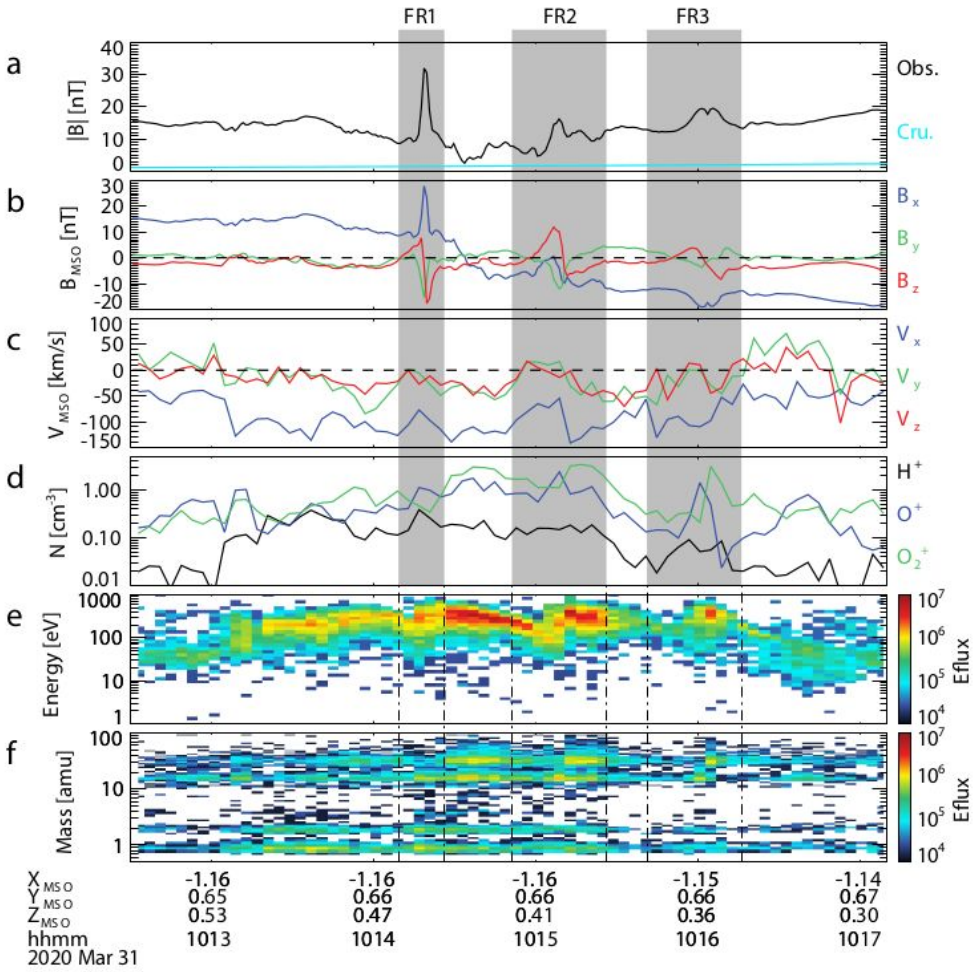

Figure 2

Overview of the current sheet crossing event in the Martian tail during 10:12:30–10:17:10 UT on 1 March 2021. The MAG measurements of (a) magnetic field strength and (b) magnetic field in the MSO frame. The STATIC measurements of (c) proton bulk velocity in the MSO frame, (d) ion number densities of , and ions, (e) energy spectra of all ion species, and (f) mass spectrum. In this study, we focus on ions with energies above 25 eV so that the spacecraft potantial and velocity have negligible effects of the moment

calculation. The X component of background magnetic field exhibited a tangential shape, consistent with the singal of a current sheet crossing. The cyan dashed line in Fig. 2b shows the modeled crustal field, which is much smaller than the measured magnetic field. Eflux in Fig. 2e–f has units of eV/cm2/str/s/eV. The marked regions denote the time interval (10:14:09-10:14:26 UT, 10:14:51-10:15:26 UT and 10:15:41-10:16:16 UT) of observed flux ropes FR1 to FR3 shown in Fig. 1a.

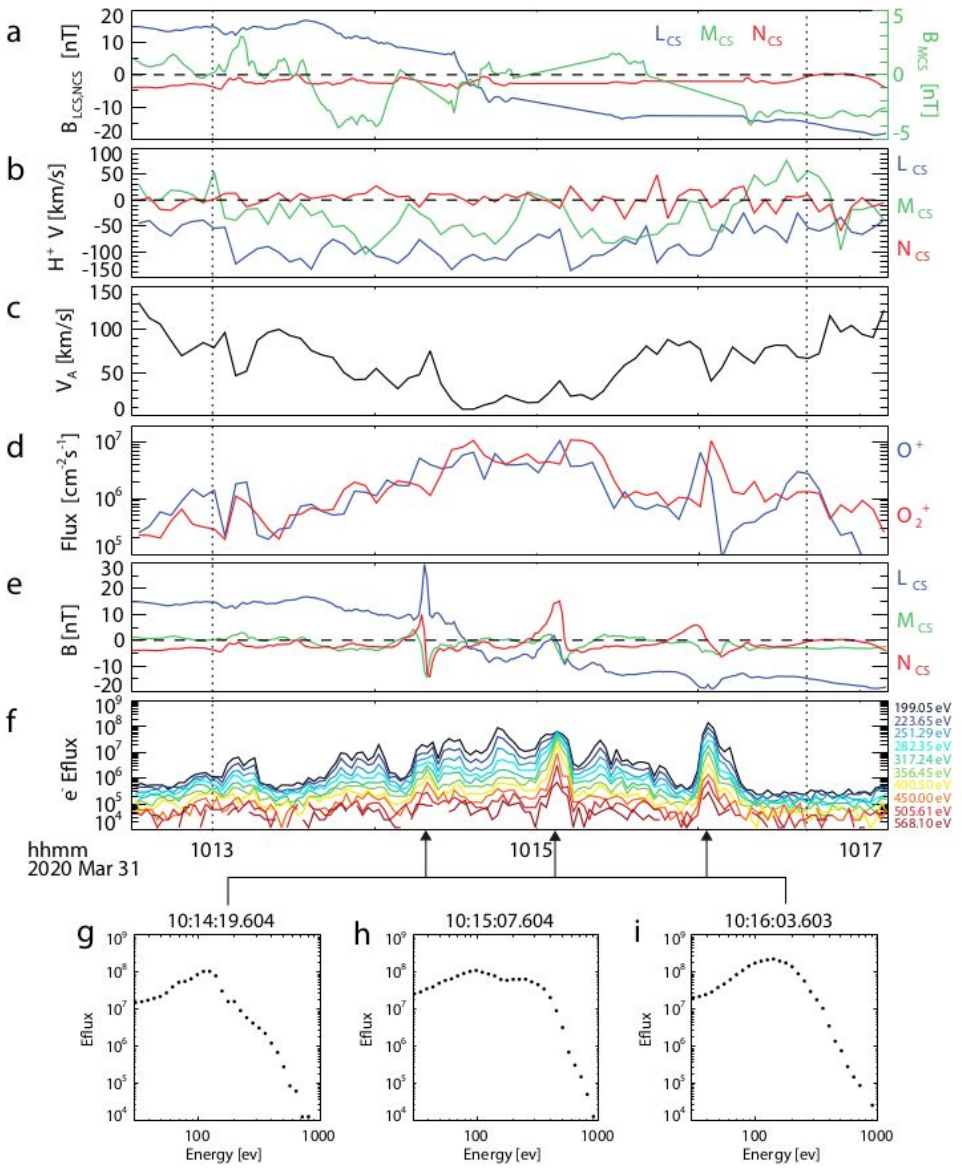

Figure 3

Magnetic and plasma measurements in the reconnection region and flux ropes. (a) Magnetic field data after removing the data within flux rope regions, as a representation of background magnetic field contributed by current sheet, (b) proton bulk velocities, (c) Alfvén velocity , where is the total ion mass density, (d) tailward fluxes (-nVX) of and , (e) original magnetic field data in the current sheet LMN coordinates. The current sheet-based minimum variance analysis is performed by the interval between two dotted lines (10:13:00-10:16:40 UT). (f) The SWEA measurements of differential energy fluxes (in units of eV/cm2/str/s/eV) of electrons with energies of 199-568 eV. (g–i) Electron distributions extracted at the time denoted by the arrows below Fig. 3f. The asymmetric Hall field, the Alfvénic outflow and the flat-top electron distribution within FR2 (Fig. 3h) suggest that FR2 was generated by local reconnection. FR1 and FR3, on the other hand, do not show an electron flat-top distribution, suggesting that they have different origins.

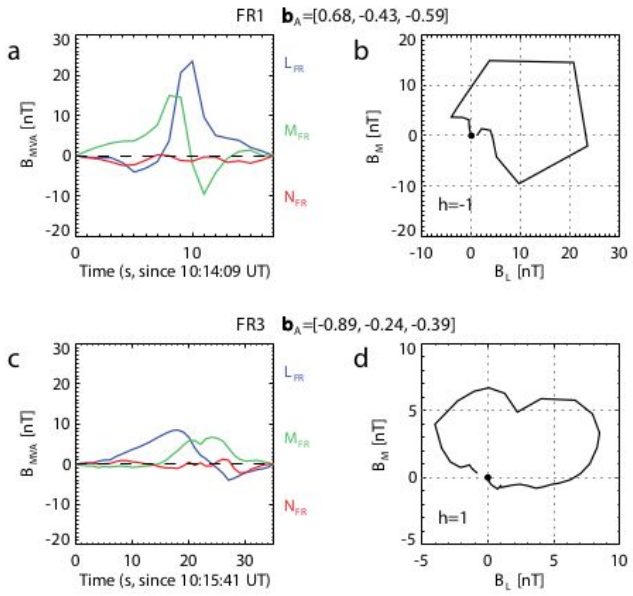

Figure 4

Magnetic measurements of flux ropes generated by boundary instabilities. (a and c) Time profiles and (b and d) hodograms of the vector magnetic field components transformed into the flux rope-based minimum variance coordinate frame after removing the current sheet signal. Black dots in Fig. 4b and 4d are the start points of the hodograms; h represents the sign of the helicity of the flux ropes. Axial orientations (relative to the MSO coordinate) of the flux ropes FR1 and FR2 were [0.68, -0.43, -0.59] and

[-0.89, -0.24, -0.39], respectively. Both axes were quasi-perpendicular (128° and 119°) to the cross-tail direction of the current sheet.

Supplementary Files

This is a list of supplementary files associated with this preprint. Click to download.

- supportinginformation.docx